Iranian Journal of Basic Medical Sciences
ijbms.mums.ac.ir

Involvement of SIRT3 downstream targets ANT1, VDAC, CYPD, and Drp1 in a rat model of hepatic encephalopathy: Therapeutic role of thymoquinone

Somayeh Hajipour [1], Mohammad Amin Dehghani [2], Alireza Sarkaki [1], Masoud Mahdavinia [2], Seyedeh Parisa Navabi [1]*

[1] Persian Gulf Physiology Research Center, Medical Basic Sciences Research Institute, Ahvaz Jundishapur University of Medical Sciences, Ahvaz, Iran
[2] Department of Toxicology, School of Pharmacy, Ahvaz Jundishapur University of Medical Sciences, Ahvaz, Iran

ARTICLE INFO

Article type:
Original

Article history:
Received: Dec 11, 2025
Accepted: May 9, 2026

Keywords:
ANT1
CYPD
DRP1
Hepatic encephalopathy
Local EEG
VDAC

ABSTRACT

Objective(s): Hepatic encephalopathy (HE) is a brain disorder linked to hyperammonemia from liver injury. Elevated ammonia levels are known to impair mitochondrial function, the primary energy source for cells. Therefore, this study aimed to evaluate energy-related signaling pathways enhancing mitochondrial biogenesis using thymoquinone (TQ) in an HE model.

Materials and Methods: Wistar rats were randomly divided into three groups: sham, HE (200 mg/kg thioacetamide (TAA) in 2ml saline, administered intraperitoneally (IP) once every 48 hr for 14 consecutive days), and HE + TQ (20 mg/kg, IP, in 2 ml DMSO 5% administered once daily for seven consecutive days). Mitochondrial biomarkers (membrane potential [MMP], oxidative stress), gene expression (AMPK, PGC-1α), and protein expression (AMPK, P-AMPK, SIRT3, ANT1, CYPD, DRP1, VDAC, and P53) were measured in brain tissue. Additionally, electroencephalogram (EEG) recordings were obtained from the dentate gyrus (DG).

Results: Our findings indicate that TQ was associated with a significant increase in MMP and a concomitant decrease in mitochondrial oxidative stress. Furthermore, TQ appeared to augment the AMPK/PGC-1α/SIRT3 signaling pathway, and was associated with the reversal of HE-induced down-regulation of ANT1 and VDAC, as well as up-regulation of CYPD, DRP1, and P53. Besides, TQ treatment was also linked to increased power recorded in the EEG from the DG region of the rat hippocampus.

Conclusion: The AMPK/PGC-1α/SIRT3 signaling pathway appears to function as a key energy sensor that may help revitalize the metabolic machinery in mitochondria, potentially facilitating metabolic exchanges and energy production, particularly in response to neurodegenerative diseases such as HE.

▶ Please cite this article as:
Hajipour S, Dehghani MA, Sarkaki AR, Mahdavinia M, Navabi SP. Involvement of SIRT3 downstream targets ANT1, VDAC, CYPD, and Drp1 in a rat model of hepatic encephalopathy: Therapeutic role of thymoquinone . Iran J Basic Med Sci 2026; 29:

Introduction

Hepatic encephalopathy (HE) is a central nervous system disorder associated with liver failure and hyperammonemia. Elevated brain ammonia levels are known to exert neurotoxic effects on energy metabolism by directly inhibiting key enzymes involved in glycolysis, the tricarboxylic acid (TCA) cycle, and the electron transport chain (ETC)—specifically affecting Coenzyme Q, complex I, and complex IV (1-3). Ammonia has also been implicated in the opening of the mitochondrial permeability transition pore (mPTP), a high-conductance channel between the inner and outer mitochondrial membranes (MIM/MOM). Prolonged mPTP opening is thought to inhibit oxidative phosphorylation and ATP synthesis, and may lead to mitochondrial swelling and membrane depolarization due to altered osmotic gradients between the mitochondrial matrix and cytosol (4-6).

AMP-activated protein kinase (AMPK) functions as an ATP sensor during energy stress. In its activated phosphorylated form, AMPK directly phosphorylates downstream target proteins that help restore energy, such as Peroxisome proliferator-activated receptor gamma coactivator 1-alpha (PGC-1α) (7). It has been reported that Sirtuin 3 (SIRT3), a downstream target of PGC-1α, plays a significant role in mediating its functions related to mitochondrial biogenesis and the regulation of reactive oxygen species (ROS)-detoxifying enzymes, including glutathione peroxidase-1 (GPx1) and superoxide dismutases (SODs) in mouse cells (8). SIRT3 has been implicated in various mitochondrial functions, including dynamics (fission and fusion), antioxidant enzymes (such as SOD2), energy metabolism (involving glycolysis, lipids, and amino acids), ATP production, respiratory chain proteins, and mitophagy (9-11).

Two key proteins involved in mitochondrial bioenergetics are the adenine nucleotide transporter type 1 (ANT1) and the voltage-dependent anion channel (VDAC), which

***Corresponding author:** Seyedeh Parisa Navabi. Persian Gulf Physiology Research Center, Medical Basic Sciences Research Institute, Ahvaz Jundishapur University of Medical Sciences, Ahvaz, Iran. Tel: +986133738248, Email: navabi.p@gmail.com

are the most abundant proteins in the MIM and MOM, respectively. ANT1 facilitates the exchange of ATP and ADP between the mitochondrial matrix and the cytoplasm, supplying ADP for ATP synthase during oxidative phosphorylation (OXPHOS) (12, 13). VDAC facilitates the transport of ions (K^+, Na^+, Ca^{2+}, Cl^-), nucleotides (ATP, ADP, AMP, NADH), and ionic metabolites (pyruvate, glutamate, succinate, malate) between the mitochondrial matrix and the cytoplasm (14). Over the past decade, the role of mitochondrial F-ATP synthase in mPTP formation has been increasingly recognized. ANT1, VDAC, and cyclophilin D are considered regulators of the mPTP and have been identified as downstream targets of SIRT3 (15).

Cyclophilin D (CypD), the only mitochondrial matrix protein from the cyclophilin family, is involved in the regulation of the mitochondrial mPTP and is thought to play a significant role in cell death following NDD. Acetylated CypD, a downstream target of SIRT3 deacetylase, has been shown to enhance mPTP opening through its interaction with F-ATP synthase (2, 4). Mitochondrial fission is a multistep process regulated by the cytosolic dynamin-related GTPase (DRP1) and its receptors, including Mff (for physiological fission) and Fis1 (for pathological fission). During physiological fission, calcium enters through VDAC and the mitochondrial Ca2+ uniporter (MCU), promoting mitochondrial contraction. Subsequently, interactions between DRP1 and Mff or Zip1 facilitate constriction and fission. Following division, mitochondria either survive or undergo autophagy, depending on the mitochondrial membrane potential (MMP), which may be normal or reduced (9, 16). A reduction in MMP during pathological conditions has been associated with excessive fission at the DRP1-Zip1 site (16). Interestingly, activation of AMPK has been reported to prevent DRP1-induced fission in mitochondria via the AMPK/DRP1 pathway (17, 18). In cases of necrosis, translocation of p53 to the mitochondria appears to be mediated by DRP1. Within the mitochondrial matrix, accumulated p53 may complex with CypD, potentially stimulating PTP opening. Additionally, p53 has been suggested to promote the expression and activation of DRP1, which could lead to mitochondrial fission (5, 19). However, under physiological conditions, p53 undergoes ubiquitination and subsequent degradation, which helps maintain its levels at a low baseline (19).

Various substances, including both chemical and natural drugs, have been shown to influence SIRT3 expression and may affect its downstream targets (11). Thymoquinone (2-isopropyl-5-methyl-1,4-benzoquinone), the active component of *Nigella sativa*, provides strong protection against oxidative damage in brain cells and hepatocytes in hepatotoxicity models induced by carbon tetrachloride or thioacetamide (TAA) (20, 21). TAA is widely used to induce hepatotoxicity and is known to have dual hepatotoxic and neurotoxic effects (22). The metabolic derivatives of TAA, including acetamide and thioacetamide-S-oxide, can bind to liver macromolecules (23), potentially leading to hyperammonemia and extensive oxidative stress. This is thought to occur through the generation of ROS, lipid peroxidation, and suppression of antioxidant defenses (24, 25). Therefore, the current study focuses on SIRT3, a master regulator of mitochondria, and its downstream mitochondrial channels/proteins (ANT1, VDAC, CypD, DRP1, and p53) involved in mitochondrial biogenesis and bioenergetics following HE and treatment with thymoquinone (TQ).

Materials and Methods

Chemicals & animals

Thymoquinone, TAA, 4-(2-hydroxyethyl)-1-piperazine-ethanesulfonic acid (HEPES), mannitol, ethylene glycol tetraacetic acid (EGTA), bovine serum albumin (BSA), malondialdehyde (MDA), Tris–HCl, tetramethoxypropane (TEP), KCl, and rhodamine 123 (Rh 123) were bought from the Sigma-Aldrich Company (St Louis, MO, USA). Sucrose and 5, 5′-dithiobis (2-nitrobenzoic acid) (DTNB) were acquired from the Merck Company (Darmstadt, Germany). Antibodies consist of β-Actin (C4) (sc-47778), m-IgGκBP-HRP (sc-5161,02), mouse anti-rabbit IgG-HRP (sc-2357), SIRT3 (F-10) (sc-365175), p53 (A-2) (sc-393031), DRP1 (C-5): sc-271583 were purchased from Santa Cruz Biotechnology, INC. AMPKα (D63G4) Rabbit mAb, Phospho-AMPKα (Thr172) (D4D6D) Rabbit mAb, ANT1/SLC25A4 antibody, and VDAC antibody were obtained from Cell Signaling Technology. ThermoScientific PageRuler Prestained Protein Ladder was purchased from Thermos Scientific. Purified anti-Cyclophilin D Antibody was purchased from Biolegend.

Thirty-three male Wistar rats (n = 11 per group), approximately 8 weeks old and weighing 200–250 g, were obtained from the central animal house of Ahvaz Jundishapur University of Medical Sciences (AJUMS, Ahvaz, Iran). The animals were housed in standard cages under controlled conditions (22 ± 2 °C, 50–60% humidity) with a 12-hr light/dark cycle (lights on at 07:00 AM). Rats had *ad libitum* access to standard commercial chow and drinking water.

Ethical approval for this study was obtained from the Ethics Committee of Ahvaz Jundishapur University of Medical Sciences (ethics code: IR.AJUMS.ABHC.REC.1399.037; grant No.: APRC-99-04). All procedures were performed in accordance with the National Institutes of Health guidelines for the care and use of laboratory animals. This study is reported in compliance with the ARRIVE (Animal Research: Reporting of *In vivo* Experiments) guidelines to ensure transparency and reproducibility.

To ensure unbiased results, the experiment was conducted under completely blinded conditions. The first experimenter administered TAA and TQ according to the protocol and placed the samples into blinded coded boxes. Brains from another group of mice were also coded prior to subsequent analyses. The second experimenter transported the coded boxes to the pharmacology laboratory for mitochondrial assessments. Finally, the third experimenter, from Avin Biotechnology Company in Ahvaz, performed real-time PCR and western blotting on the blinded samples.

Hepatic encephalopathy model and experimental design

Animals were included in the study if they successfully underwent the HE model induction. The HE model, along with the effective dose of TQ and the behavioral and blood biochemical assessments, was validated in our previous studies (26, 27). Briefly, thioacetamide (TAA) (200 mg/kg, dissolved in 2 ml of sterile 0.9% saline solution) was administered intraperitoneally once every 48 hr for 14 consecutive days to induce both acute liver failure and acute HE.

For the experimental design, rats were randomly divided into three main groups. Random numbers were generated using a standard function in Microsoft Excel to assign treatments to the Wistar rats.

1. **Sham**: Received vehicles only.
2. **HE**: Received TAA (200 mg/kg in 2 ml saline, IP) once every 48 hr for 14 consecutive days.
3. **HE + TQ20**: Received TQ (20 mg/kg in 2 ml saline containing 5% DMSO, IP) for 7 consecutive days, starting 24 hr after the last TAA injection.

In each group, six rats were used for hippocampal local EEG and mitochondrial marker measurements, while five rats were designated for gene and protein expression analysis in brain tissue. All electrophysiological and biochemical assays were performed after the last TQ injection.

Isolation of mitochondria and measurement of its markers

Euthanasia was performed on the rats using deep anesthesia induced by intraperitoneal injection of thiopental at a dose of 50 mg/kg. Following anesthesia induction, the animals were euthanized by decapitation using a guillotine to ensure rapid and humane euthanasia. Subsequently, the brains were quickly removed for molecular experiments to minimize tissue degradation and preserve sample integrity.

The brains were washed in saline and homogenized in an ice-cooled buffer containing 75 mM mannitol, 220 mM sucrose, 0.5 mM EGTA, 2 mM HEPES, and 0.1% BSA (pH 7.4) at a 10:1 buffer-to-tissue (v/w) ratio. To remove cell debris and nuclei, the homogenate was centrifuged at 1,000 × g for 10 min at 4 °C. The resulting supernatant was re-centrifuged under the same conditions to collect the heavy membrane fractions enriched in mitochondria.

The mitochondrial pellet was then resuspended in fresh isolation buffer and centrifuged again at 12,300 × g for 10 min at 4 °C. Finally, the mitochondrial protein concentration was adjusted to 0.5 mg/ml using the Coomassie Brilliant Blue protein assay, with bovine serum albumin (BSA) as the standard (28).

Mitochondrial membrane potential (MMP, $\Delta\Psi_m$)

Mitochondrial membrane potential (MMP) was assessed by measuring the uptake of the fluorescent dye rhodamine 123 (Rh123, 10 µM) using a fluorescence spectrophotometer (Shimadzu RF-5000U; λEx = 490 nm, λEm = 534 nm). Briefly, mitochondrial fractions (0.5 mg protein/ml) were incubated with rhodamine 123 in a buffer containing 125 mM sucrose, 65 mM KCl, and 10 mM HEPES (pH 7.2) for 30 min at 37 °C. Fluorescence intensity was then measured using a multifunctional fluorescent microplate reader at excitation and emission wavelengths of 485 nm and 525 nm, respectively (29).

Mitochondrial ROS and MDA levels

Mitochondrial ROS levels in isolated brain mitochondria were assessed by measuring the fluorescence intensity of 10 µM DCFH (2,7-dichlorofluorescein). Briefly, mitochondria were incubated in a respiratory buffer containing 125 mM sucrose, 65 mM KCl, 10 mM HEPES, 20 µM Ca^{2+}, and 5 mM sodium succinate (pH 7.2). DCFH-DA was then added, and the samples were incubated at 37 °C in the dark for 30 min. ROS levels were subsequently measured using a fluorescence spectrophotometer (Shimadzu RF-5000U; λEx = 488 nm, λEm = 527 nm).

Lipid peroxidation was evaluated by measuring malondialdehyde (MDA) levels in isolated brain mitochondria using the thiobarbituric acid reactive substances (TBARS) assay. Briefly, mitochondrial fractions (0.2 ml) were mixed with 0.3 ml of 0.2% thiobarbituric acid (TBA), 0.25 ml of sulfuric acid, and 15% (w/v) trichloroacetic acid. The mixture was boiled at 100 °C for 30 min, then cooled on ice. Subsequently, 0.4 ml of n-butanol was added to each tube. After centrifugation at 15,000 × g for 1 min, the absorbance of the supernatant was measured at 532 nm using an ELISA reader (Tecan, Rainbow Thermo, Austria). MDA levels were expressed as nmol/mg protein, based on a standard curve prepared with tetramethoxypropane (TEP)

Mitochondrial CAT, SOD, and GPX measurement

Mitochondrial catalase (CAT) activity was determined by incubating the mitochondrial suspension with Tris-HCl (0.05 mM) and H_2O_2 (0.01 M) for 10 min. After incubation, ammonium molybdate (4%) was added, and the absorbance of the mixture was measured at 410 nm. CAT activity was expressed as U/mg protein. Mitochondrial SOD and glutathione peroxidase (GPx) activities were assessed using standard diagnostic kits (Zellbio Company, Germany) according to the manufacturer's instructions (30, 31).

Real-time polymerase chain reaction

Total RNA was extracted from homogenized brain tissues, and its concentration and purity were assessed by measuring optical density at 260/280 nm using a NanoDrop spectrophotometer (Pishro Pajoohesh, Iran). For each sample, 5 µl of RNA was used for quality control. Complementary DNA (cDNA) was synthesized using a Takara cDNA synthesis kit according to the manufacturer's instructions. The reaction mixture (10 µl final volume) contained 0.5 µl PrimeScript RT Enzyme Mix I, 2 µl PrimeScript Buffer, 0.5 µl Random 6 mers, and 500–1000 ng of RNA, adjusted with RNase-free distilled water. The mixture was incubated in a thermocycler under the following conditions: 37 °C for 15 min, 85 °C for 5 sec, and then held at 4 °C. Real-time PCR was performed in duplicate using a RunMei Q200 (China) thermal cycler. Each 12.5 µl reaction contained 0.5 µl of specific primers (Table 1), 1 µl ROX dye, 6.25 µl SYBR Green qPCR Master Mix (2×), 2.75 µl RNase-free water, and 3 µl of cDNA template. The amplification protocol consisted of 50 cycles under the following conditions: initial denaturation at 94 °C for 5 min, followed by 94 °C for 15 sec (denaturation), 60 °C for 15 sec (annealing), and 72 °C for 30 sec (extension), in accordance with the SYBR YT4500 RT-PCR Kit instructions. Relative gene expression levels were calculated using the comparative threshold cycle ($2^{-\Delta\Delta Ct}$) method with RunMei QC3.2 software.

Western blot analysis

Frozen brain tissue samples were homogenized in 20 ml of lysis buffer containing 0.1% Triton X-100 or SDS, 50 mM Tris-HCl (pH 7.5), 0.25% sodium deoxycholate, 150 mM NaCl, 1 mM EDTA, and a protease inhibitor cocktail (10×). The homogenates were then centrifuged at 14,000 × g for 10 min at 4 °C, and protein concentrations were determined

Table 1. Forward and reverse primer sequences used for RT-PCR amplification of AMPK and PGC-1α in male Wistar rats

Gene name	Forward primer	Reverse primer
β-Actin	TCTACAATGAGCTGCGTGTG	AGGTCTCAAACATGATCTGGGT
AMPK	GATAGCTGACTTCGGACTCTCT	AGGATAACACCACAGCTCCA
PGC-1α	GCAACATGCTCAAGCCAAAC	TGCAGTTCCAGAGAGTTCCA

using a BCA Protein Assay Kit. Equal amounts of protein were separated by 10% SDS-PAGE and transferred onto nitrocellulose membranes. The membranes were blocked overnight at 4 °C in blocking buffer, followed by incubation for one hour with the following mouse monoclonal antibodies: anti-AMPK, anti-P-AMPK, anti-SIRT3, anti-P53, anti-ANT1, anti-CYPD, anti-DRP1, anti-VDAC, and anti-β-actin (all diluted 1:2000). After washing, the membranes were incubated for one hour with an HRP-conjugated rabbit polyclonal anti-mouse secondary antibody (diluted 1:2000 in PBS). Immunoreactive bands were visualized using an electrochemiluminescence (ECL) kit (Abcam, 133408, USA) and scanned with a JS 2000 scanner (BonninTech, China). Band intensities were quantified using the IMAGE JS 2000 (32).

Local EEG recording

Rats were anesthetized with ketamine/xylazine (100/10 mg/kg, IP) and positioned in a stereotaxic apparatus. A small burr hole was drilled in the skull, and a stainless steel, Teflon-coated EEG electrode (bare diameter: 0.005", coated diameter: 0.008"; A-M Systems, Inc., WA, USA) was implanted into the dentate gyrus (DG) region of the left hippocampus. The stereotaxic coordinates were as follows: anteroposterior (AP): −3.8 mm from bregma, mediolateral (ML): ±3.5 mm, and dorsoventral (DV): −4.0 mm from the skull surface.

Local field potentials (EEG) were recorded using a ML135 bioamplifier connected to a 4-channel data acquisition system (PowerLab, AD Instruments, Australia) and analyzed with LabChart software (version 7). Signals were amplified 1,000×, sampled at 400 Hz, and band-pass filtered between 0.3 and 70 Hz. For each animal, recordings were performed for 5 min. Power spectral analysis was conducted on three 5-second artifact-free epochs. The absolute power (μV^2/Hz) of the crude EEG (0.3–70 Hz) and its frequency sub-bands—delta (0.5–4 Hz), theta (4–8 Hz), alpha (8–12 Hz), beta (12–30 Hz), and gamma (30–70 Hz)—were calculated and compared between experimental groups (33).

Statistical analysis

Statistical analyses were performed using GraphPad Prism (version 8.02, GraphPad, San Diego, CA, USA). All data are presented as mean ± standard error of the mean (SEM). A one-way analysis of variance (ANOVA) followed by Bonferroni's *post hoc* test was used to compare differences among the experimental groups. A *P*-value of less than 0.05 was considered statistically significant.

Results

Mitochondrial oxidative stress

Analysis of mitochondrial membrane damage, ROS levels, and MDA content revealed a significant increase in the HE group compared to the sham group ($P<0.001$). In contrast, treatment with TQ (20 mg/kg) significantly attenuated these parameters relative to the HE group ($P<0.001$) (Figure 1A–C).

As shown in Figure 1D–F, mitochondrial antioxidant enzyme activities, including SOD, CAT, and GPx, were significantly decreased in the HE group compared to the sham group ($P<0.001$). However, administration of TQ (20 mg/kg) significantly restored the activities of these enzymes compared to the HE group ($P<0.001$).

Real time PCR

One-way ANOVA revealed a significant decrease in the expression of AMPK ($P=0.003$) and PGC-1α ($P<0.001$) in the HE group compared to the sham group. In contrast, treatment with TQ (20 mg/kg) significantly increased the expression of both AMPK ($P=0.004$) and PGC-1α ($P=0.001$) compared to the HE group. (Figure 2A, B).

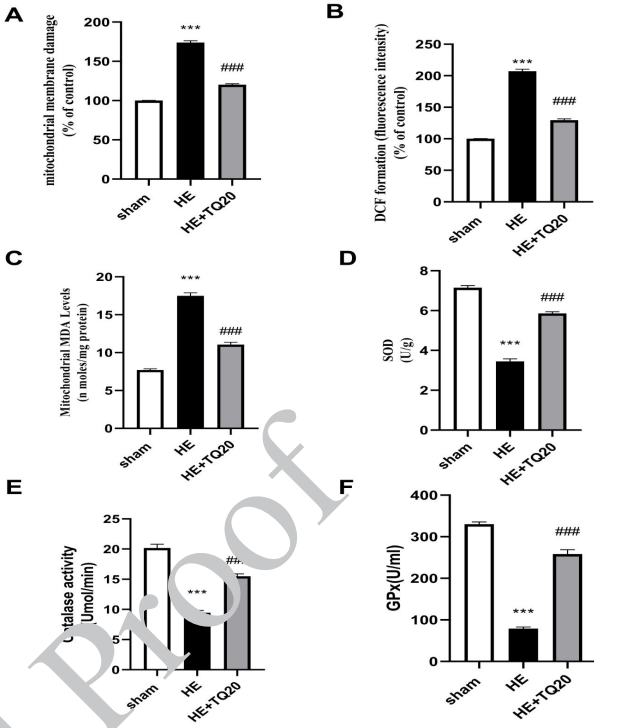

Figure 1. Effects of TQ treatment (20 mg/kg in 2 ml DMSO 5%, IP, 7 day) were assessed 24 hr after the last injection of TAA (200 mg/kg in 2 ml saline, IP, once every 48 hr for 14 consecutive days) on the damage level of mitochondrial membrane (A), ROS level (B), MDA level (C), SOD (D), CAT (E), and GPx (F) in the brain tissue of HE rat model. One-way ANOVA followed by Bonferroni's post hoc test multiple comparisons was applied for analysis. Data are presented as mean ± SEM (n = 6); **P*<0.05, ***P*<0.01, ****P*<0.001, vs sham; and #*P*<0.05, ##*P*<0.01, ###*P*<0.001, vs HE group.
TQ: Thymoquinone; IP: Intraperitoneally; TAA: Thioacetamide; ROS: Reactive oxygen species; MDA: Malondialdehyde; SOD: Superoxide dismutases; CAT: Catalase; GPx: Glutathione peroxidase; HE: Hepatic encephalopathy

Western blot

As shown in Figure 3, the protein levels of SIRT3, ANT1, and VDAC were significantly decreased in the HE group compared to the sham group ($P<0.001$, $P=0.002$, and $P=0.001$, respectively). Conversely, treatment with TQ (20

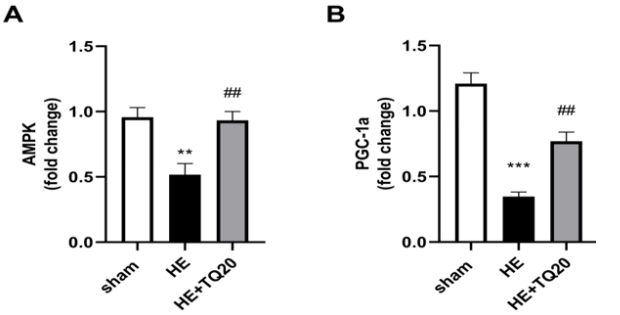

Figure 2. The effectsEffects of TQ treatment (20 mg/kg in 2 ml DMSO 5%, IP, 7 day) were assessed 24 hr after the last injection of TAA (200 mg/kg in 2 ml saline, IP, once every 48 hr for 14 consecutive days) on the gene expression of AMPK (A) and PGC-1α (B) in the brain tissue of HE rat model. One-way ANOVA followed by Bonferroni's *post hoc* test multiple comparisons was applied for analysis. Data are presented as mean ± SEM (n = 5); **P*<0.05, ***P*<0. 01,***, ****P*<0. 001, vs. sham; and #*P*<0.05, ##*P*<0.01, ###*P*<0.001, vs. HE group.
TQ: Thymoquinone; IP: Intraperitoneally; TAA: Thioacetamide; HE: Hepatic encephalopathy

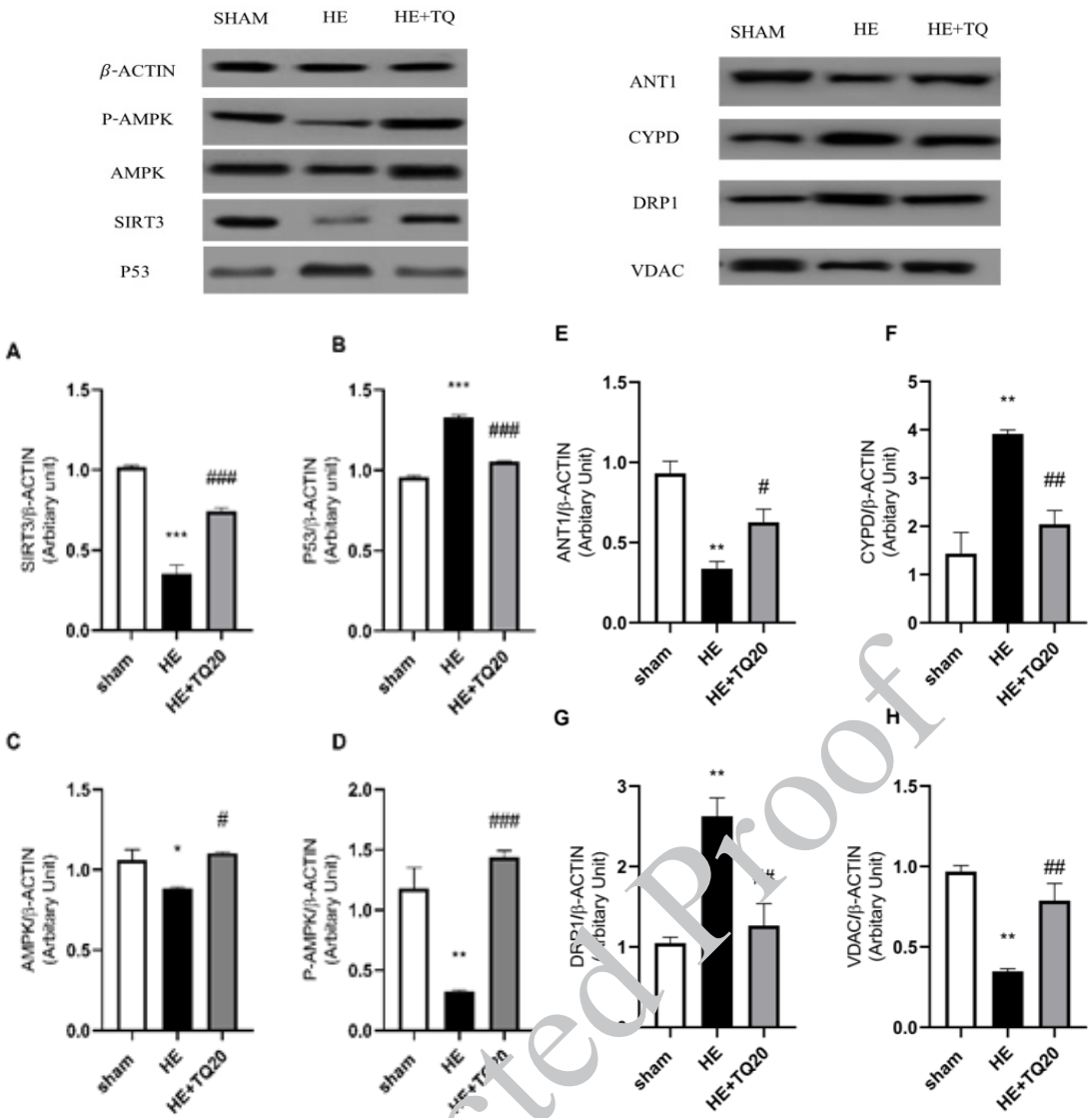

Figure 3. Effects of TQ treatment (20 mg/kg in 2 ml DMSO 5% IP, 1 hr) were assessed 24 hr after the last injection of TAA (200 mg/kg in 2 ml saline, IP, once every 48 hr for 14 consecutive days) on the protein expression of SIRT3 (A), P53 (B), AMPK (C), P-AMPK (D), ANT1(E), CYPD (F), DRP1(G), and VDAC (H) in the brain tissue of HE rat model. One-way ANOVA followed by Bonferroni's *post hoc* test multiple comparisons was applied for analysis. Data are presented as mean ± SEM (n = 3); **P*<0.05, ***P*<0.01,****P*<0.001, vs sham group; #*P*<0.05, ##*P*<0.01, ###*P*<0.001, vs HE group.
TQ: Thymoquinone; IP: Intraperitoneally; TAA: Thioacetamide; HE: Hepatic encephalopathy; SIRT3: Sirtuin 3; CYPD: Cyclophilin D; DRP1: Dynamin-related GTPase; VDAC: Voltage-dependent anion channel

mg/kg) significantly increased the levels of these proteins compared to the HE group (*P*<0.001, *P*=0.049, and *P*=0.007, respectively).

In contrast, the expression levels of P53 (*P*<0.001), CYPD (*P*=0.002), and DRP1(*P*=0.004) were significantly increased in the HE group relative to the sham group, while TQ treatment significantly reduced their levels compared to the HE group (*P*<0.001, *P*=0.010, and *P*=0.007, respectively) (Figure 3).

Western blot analysis further revealed a significant decrease in AMPK and P-AMPK protein levels in the HE group compared to the sham group (*P*<0.05 and *P*<0.01, respectively). Treatment with TQ (20 mg/kg) significantly up-regulated AMPK and P-AMPK expression compared to the HE group (*P*<0.05 and *P*<0.001, respectively).

Electrophysiology

Representative local EEG recordings from the hippocampal DG region are shown in Figure 4. As illustrated in Figure 5, total EEG power was significantly decreased in the HE group compared to the sham group (*P*<0.001), and significantly increased following TQ treatment compared to the HE group (*P*=0.04).

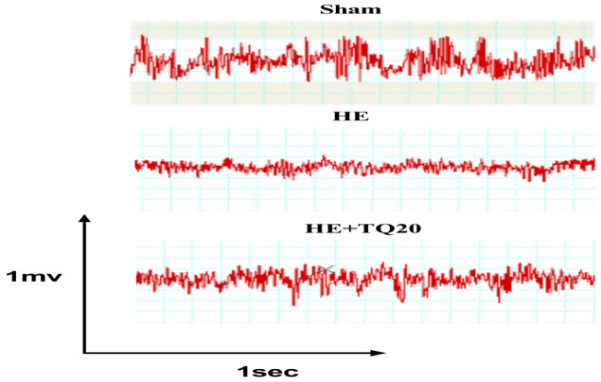

Figure 4. A sample of amplified crude EEG waves from hippocampus DG region in three main rat groups
EEG: Electroencephalogram; DG: Dentate gyrus

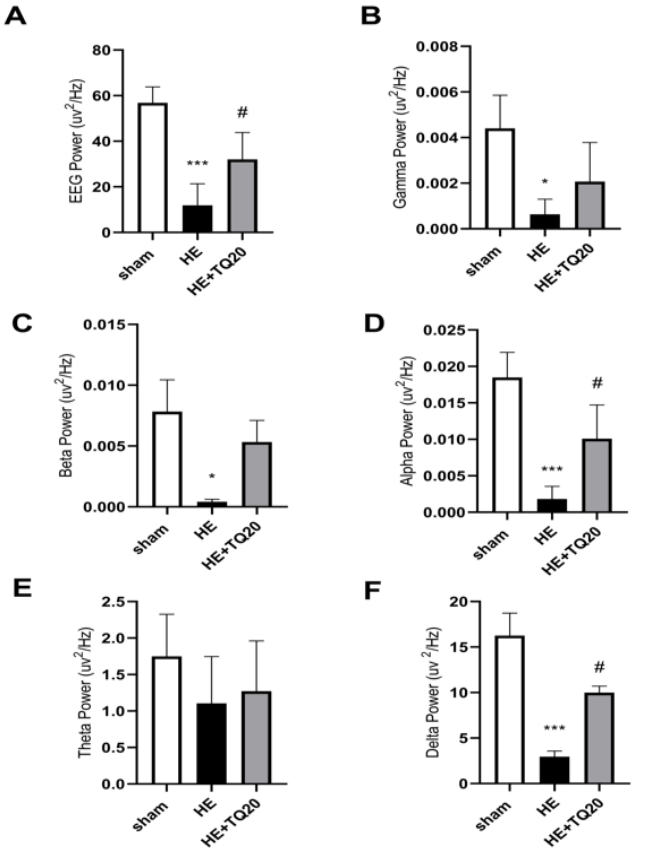

Figure 5. Effects of TQ treatment (20 mg/kg in 2 ml DMSO 5%, IP, 7 day) were assessed 24 hr after the last injection of TAA
(200 mg/kg in 2 ml saline, IP, once every 48 hr for 14 consecutive days) on the local EEG in the hippocampus and its frequency band powers (uv2/Hz) in EEG crude (A), Gamma power (B) Beta power (C) Alpha power (D) Theta power (E) and Delta power (F) of HE rat model. One-way ANOVA followed by Bonferroni's *post hoc* test multiple comparison was applied for analysis. Data are presented as mean ± SEM (n = 6); **P*<0.05, ***P*<0.01, ****P*<0.001, vs sham and #*P*<0.05, ##*P*<0.01, ###*P*<0.001, vs HE group.
TQ: Thymoquinone; IP: Intraperitoneally; TAA: Thioacetamide; EEG: Electroencephalogram; E: Hepatic encephalopathy

Analysis of frequency sub-bands revealed significant reductions in the HE group compared to the sham group across all bands: gamma (P=0.03), beta (P=0.02), alpha and delta (P<0.001). Treatment with TQ (20 mg/kg) increased the power of all frequency bands, with statistically significant elevations observed in the alpha (P=0.04) and delta (P=0.01) bands compared to the HE group.

Discussion

HE is a neurological dysfunction associated with severe liver disease, in which ammonia is considered to play a principal role as a key neurotoxin. Ammonia is thought to sensitize the brain to oxidative stress and various destructive factors (34). Excessive ammonia in the brain may disrupt mitochondrial function—which serves as both the primary energy source and a significant source of ROS—by interfering with the ETC or specific proteins within it. Consequently, the brain in HE may experience ATP deficits, referred to as energy stress. This phenomenon is sensed by AMPK as an energy stressor. However, current findings suggest that the compensatory response of AMPK in the HE model may be insufficient to up-regulate the protective protein SIRT3, potentially contributing to significant mitochondrial dysfunction. For instance, we observed the down-regulation of two important bioenergetic proteins, ANT1 and VDAC, alongside the up-regulation of two degrading proteins, CypD and DRP1, as well as p53 in the brains of HE rats. Additionally, MMP was found to be decreased, and oxidative stress in mitochondria appeared to be increased following HE induction, as evidenced by a decrease in SOD, catalase (CAT), and GPx activities, along with an increase in MDA levels. In the subsequent treatment phase, TQ (20 mg/kg) was observed to significantly reverse these effects by amplifying the AMPK/PGC-1α/SIRT3 signaling pathway and was associated with improved electroencephalogram readings recorded from the DG region.

Mitochondrial dysfunction in the brain is commonly characterized by decreased MMP, reduced activity of antioxidant enzymes, increased opening of the mitochondrial mPTP, elevated levels of reactive oxygen species (ROS), and excessive mitochondrial fission (9, 35). In this regard, Chadipiralla *et al.* (2012) reported a significant increase in mitochondrial swelling in the cortical region of rat brains following thioacetamide-induced HE (36). Additionally, cultured astrocytes have been shown to exhibit ammonia-induced mitochondrial swelling associated with oxidative stress (37, 38). According to Bustamante *et al.* (2011), hyperammonemia may trigger mitochondrial dysfunction through mechanisms such as electron transport chain (ETC) locking, opening of the mPTP, release of cytochrome c, and collapse of the transmembrane potential. These events may subsequently contribute to hippocampal apoptosis in the HE model (39). However, the primary aspect of brain injury following neurodegenerative diseases (NDD) is thought to be associated with the opening of the mPTP (40, 41). Due to the direct effects of ammonia on brain mitochondria, it has been suggested as a potential target for managing HE (1).

It is well established that the pathogenesis of most NDDs is believed to originate from disrupted mitochondrial ATP synthesis (3). Activation of brain AMP-activated protein kinase (AMPK) has been observed as a compensatory response to liver failure following bile duct ligation (BDL) or thioacetamide (TAA) injection, suggesting that brain energy deficit may play a significant role in the development of HE (42).

In agreement with our study, Sedik *et al.* (2024) reported that the suppression of the AMPK/SIRT1 pathway following thioacetamide (TAA) administration was associated with neuronal death. Conversely, activation of AMP-activated protein kinase (AMPK) was linked to memory improvement in bile duct ligation-induced HE (43). Additionally, both protein and mRNA levels of SIRT3 have been reported to be significantly down-regulated in NDDs, including HE (9, 35, 44). Several studies in the context of NDDs suggest that SIRT3 may inhibit mitochondrial permeability transition pore (mPTP) opening through deacetylation of cyclophilin D (CypD), thereby reducing cytochrome c release and subsequent apoptosis (45). Supporting this, Yan *et al.* (2022) demonstrated that SIRT3 overexpression in the spinal cord attenuated mitochondrial dysfunction and oxidative stress in a spinal cord injury model, as reflected by decreased mPTP opening and MDA levels, along with increased SOD activity and mitochondrial membrane potential (MMP) (35).

According to Argueti-Ostrovsky's discussion in 2024, the expression of voltage-dependent anion channel (VDAC) has been reported to significantly decrease in certain NDDs, such as Parkinson's disease and amyotrophic lateral sclerosis (46). This reduction is thought to impair the conductance

of ions and metabolites across VDAC, an event that may correlate with decreased energy production. Consequently, this could contribute to the activation of intrinsic apoptotic pathways and subsequent mitochondrial dysfunction (14). Furthermore, Ding *et al.* found that the levels of soluble adenine nucleotide translocator 1 (ANT1) were significantly decreased in several regions of the brain, including the midbrain, striatum, hippocampus, cerebellum, and brainstem, in a rat model of Parkinson's disease (47). It has been suggested that transgenic overexpression of ANT1 reduces oxidative stress, decreases cytochrome c release from mitochondria, increases cell survival, and stabilizes the MMP in ischemic cardiomyocytes (48). According to Zhang *et al.* nuclear factor kappa B (NF-κB) signaling has been shown to repress ANT1, the most abundant protein in the mitochondrial inner membrane. This repression is thought to induce mitochondrial dysfunction, potentially by impairing ATP/ADP exchange, reducing ATP production, and affecting proton conductance. Furthermore, it may promote the opening of the mitochondrial mPTP through calcium overload (49).

On the other hand, in NDD models such as Alzheimer's disease, excessive mitochondrial fragmentation has been suggested to result from a high interaction between dynamin-related protein 1 (Drp1) and fission 1 protein (Fis1), potentially leading to mitochondrial dysfunction (16). In this context, inhibition of Drp1 has been associated with reduced cortical injury, decreased mitochondrial fragmentation, improved blood-brain barrier (BBB) permeability, diminished ATP reduction, prevention of synaptic failure, preservation of MMP, reduced hippocampal atrophy, and enhanced neurogenesis in the DG region (50, 51).

Regarding the AMPK/Drp1 axis, several studies have indicated that AMPK activators can alleviate levels of SOD, MMP, and ATP, while also decreasing MDA, ROS levels, and mitochondrial fission potentially mediated by Drp1 activation or the expression of mitochondrial fission genes, including mitochondrial fission factor (Mff) and Fis1. This effect is thought to be mediated via the AMPK/Drp1 axis (17, 18, 52, 53). According to the findings of Liu *et al.* (2018), inhibition of AMPK activity has been associated with the reactivation of Drp1, which may abolish the normalizing effect of SIRT3 on the AMPK/Drp1 axis and mitochondrial fission (54). Other reports have also suggested that the interaction between Drp1 and p53 may stabilize and translocate p53 to the mitochondria, potentially promoting apoptosis through the interaction of p53 with CypD and the opening of the mPTP (55, 56).

It has been reported that BBB impairment in sepsis or HE may be mediated through the activation of the Drp1-Fis1 pathway, potentially leading to mitochondrial dysfunction and the enhancement of vascular permeability regulators (57, 58). In sepsis-associated encephalopathy, SIRT3-mediated deacetylation of CypD has been found to be significantly diminished, an event that has been associated with the opening of the mPTP and subsequent mitochondrial apoptosis in the hippocampus of mice (59). The Drp1 peptide inhibitor (P110) has been shown to block the interaction between Drp1 and Fis1, effectively abolishing excessive mitochondrial fission and neurotoxicity in cultured neurons. Additionally, P110 has been reported to reduce p53 recruitment to the mitochondria and decrease infarction volume in the brains of ischemic rats (19, 60).

In agreement with our EEG data from the DG region of the hippocampus, Khanna *et al.* (2020) highlighted the progressive role of SIRT1 activation in influencing the dendritic length and arborization of CA1 pyramidal neurons, a feature considered crucial for long-term potentiation (LTP) in electroencephalogram readings and neurobehavioral outcomes in a model of HE (61). Additionally, activation of SIRT3 has also been suggested to restore ammonia-induced mitochondrial dysfunction in the hippocampus of rats with HE (44).

Conclusion

Based on our findings, it is possible that the HE condition may induce impairment in the mitochondrial exchange of ATP/ADP, nucleotides, ions, or metabolites through adenine nucleotide translocator 1 (ANT1) and voltage-dependent anion channel (VDAC) between the mitochondrial matrix and cytosol, potentially leading to mitochondrial dysfunction. Additionally, we observed up-regulation of dynamin-related protein 1 (Drp1), cyclophilin D (CypD), and p53, which is thought to induce excessive mitochondrial fission and the opening of the mitochondrial mPTP. However, the question remains whether these effects are directly mediated by hyperammonemia, a key feature of HE.

Acknowledgment

This study was supported by a grant (APRC-9904) from the Physiology Research Center, Ahvaz Jundishapur University of Medical Sciences, Ahvaz, Iran.

Limitation

Several limitations of the present study should be acknowledged and addressed in future research. First, while our findings support a mechanistic link between the AMPK/PGC-1α/SIRT3 pathway and the observed protective effects, further investigations—such as those employing specific inhibitors, siRNA knockdown, or knockout models of SIRT3, AMPK, or PGC-1α—are required to conclusively establish this axis as the underlying mechanism of action. Second, the direct effects of ammonia on mitochondrial function need to be examined in controlled *in vitro* settings. Third, future studies should also aim to assess mitochondrial mPTP currents *in vivo* to better understand the electrophysiological consequences of mitochondrial dysfunction in the context of HE.

Funding

The work was funded by the Ahvaz Jundishapur University of Medical Sciences (AJUMS, grant No.: APRC-99-04).

Ethical Approval

The study was performed in accordance with the guidelines of the Ethics committee of Ahvaz Jundishapur University of Medical Sciences, Ahvaz, Iran (ethic code: IR.AJUMS.ABHC.REC.1399.037).

Accessibility of Data

The data that support the findings of this study are available from the corresponding author upon reasonable request.

Authors' Contributions

S H and MA D performed experiments and collected

data. A S and M M directed and managed the study. SP N designed the research, supervised, and wrote the main manuscript. All authors reviewed the manuscript.

Conflicts of Interest

The authors have no conflicts of interest.

Declaration

The authors acknowledge the use of the Monica artificial intelligence tool for grammatical editing and English language enhancement of the present manuscript. All scientific content, data analysis, and conclusions are the sole work of the authors

References

1. Heidari R. Brain mitochondria as potential therapeutic targets for managing hepatic encephalopathy. Life Sci 2019; 218: 65-80.
2. Fayaz SM, Raj YV, Krishnamurthy RG. CypD: The key to the death door. CNS Neurol Disord Drug Targets 2015; 14: 654-663.
3. Prasad SK, Acharjee A, Singh VV, Trigun SK, Acharjee P. Modulation of brain energy metabolism in hepatic encephalopathy: Impact of glucose metabolic dysfunction. Metab Brain Dis 2024; 39: 1649-1665.
4. Coluccino G, Muraca VP, Corazza A, Lippe G. Cyclophilin D in mitochondrial dysfunction: A key player in neurodegeneration? Biomolecules 2023; 13: 1265:1-30
5. Dashzeveg N, Yoshida K. Cell death decision by p53 via control of the mitochondrial membrane. Cancer Lett 2015; 367: 108-112.
6. Kumarswamy R, Chandna S. Putative partners in Bax mediated cytochrome-c release: ANT, CypD, VDAC or none of them? Mitochondrion 2009; 9: 1-8.
7. Herzig S, Shaw RJ. AMPK: Guardian of metabolism and mitochondrial homeostasis. Nat Rev Mol Cell Biol 2018; 19: 121-135.
8. Kong X, Wang R, Xue Y, Liu X, Zhang H, Chen Y, *et al.* Sirtuin 3, a new target of PGC-1α, plays an important role in the suppression of ROS and mitochondrial biogenesis. PLoS One 2010; 5: e11...
9. Meng H, Yan WY, Lei YH, Wan Z, Hou YY, Sun LK, *et al.* SIRT3 regulation of mitochondrial quality control in neurodegenerative diseases. Front Neurosci 2019; 11:313.
10. Sidorova-Darmos E, Sommer R, Eubanks J. The role of SIRT3 in the brain under physiological and pathological conditions. Front Cell Neurosci 2018; 12: 196.
11. Yang H, Zhou Z, Liu Z, Chen J, Wang Y. Sirtuin-3: A potential target for treating several types of brain injury. Front Cell Dev Biol 2023; 11:1154831.
12. Atlante A, Valenti D, Latina V, Amadoro G. Dysfunction of mitochondria in Alzheimer's disease: ANT and VDAC interact with toxic proteins and aid to determine the fate of brain cells. Int J Mol Sci 2022; 23: 7722.
13. Sharer JD. The adenine nucleotide translocase type 1 (ANT1): A new factor in mitochondrial disease. IUBMB Life 2005; 57: 607-614.
14. Argueti-Ostrovsky S, Barel S, Kahn J, Israelson A. VDAC1: A key player in the mitochondrial landscape of neurodegeneration. Biology (Basel) 2024; 15: 33.
15. Coluccino G, Negro A, Filippi A, Bean C, Muraca VP, Gissi C, *et al.* N-terminal cleavage of cyclophilin D boosts its ability to bind F-ATP synthase. Commun Biol 2024; 7: 1486.
16. Shi W, Tan C, Liu C, Chen D. Mitochondrial fission mediated by Drp1-Fis1 pathway and neurodegenerative diseases. Rev Neurosci 2023; 34: 275-294.
17. Hao L, Shi M, Ma J, Shao S, Yuan Y, Liu J, *et al.* A cholecystokinin analogue ameliorates cognitive deficits and regulates mitochondrial dynamics via the AMPK/Drp1 pathway in APP/PS1 mice. CNS Neurosci Ther 2024; 11: 382-401
18. Li J, Wang Y, Wang Y, Wen X, Ma XN, Chen W, *et al.* Pharmacological activation of AMPK prevents Drp1-mediated mitochondrial fission and alleviates endoplasmic reticulum stress-associated endothelial dysfunction. Biochem Pharmacol 2015; 86: 62-74.
19. Guo X, Sesaki H, Qi X. Drp1 stabilizes p53 on the mitochondria to trigger necrosis under oxidative stress conditions *in vitro* and *in vivo*. Biochem J 2014; 461: 137-146.
20. Hajipour S, Farbood Y, Dianat M, Rashno M, Khorsandi LS, Sarkaki A. Thymoquinone improves behavioral and biochemical deficits in hepatic encephalopathy induced by thioacetamide in rats. Neurosci Lett 2021; 745: 135617.
21. Nagi MN, Alam K, Badary OA, Al-Shabanah OA, Al-Sawaf HA, Al-Bekairi AM. Thymoquinone protects against carbon tetrachloride hepatotoxicity in mice via an anti-oxidant mechanism. IUBMB Life 1999; 47: 153-159.
22. Sedik AA, Hussein DT, Fathy K, Mowaad NA. Neuroprotective and cognitive enhancing effects of herbecetin against thioacetamide induced hepatic encephalopathy in rats via upregulation of AMPK and SIRT1 signaling pathways. Sci Rep 2024; 14: 11396.
23. Swapna I, Kumar KSS, Reddy NVB, Murthy CR, Reddanna P, Senthilkumaran B. Phospholipid and cholesterol alterations accompany structural disarray in myelin membrane of rats with hepatic encephalopathy induced by thioacetamide. Neurochem Int 2006; 49: 238-244.
24. Butterworth RF. Hepatic encephalopathy: A central neuroinflammatory disorder? Hepatology 2011; 53:1372-1376.
25. Sathyasaikumar K, Swapna I, Reddy P, Murthy CR, Roy K, Gupta AD, *et al.* Co-administration of C-phycocyanin ameliorates thioacetamide-induced hepatic encephalopathy in Wistar rats. J Neurol Sci 2007; 2...: 67-75.
26. Hajipour S, Farbood Y, Dianat M, Rashno M, Khorsandi LS, Sarkaki A. Thymoquinone improves cognitive and hippocampal long-term potentiation deficits due to hepatic encephalopathy in rats. Iran J Basic Med Sci 2021; 24:881.
27. Hajipour S, Farbood Y, Dianat M, Rashno M, Khorsandi LS, Sarkaki A. Thymoquinone improves behavioral and biochemical deficits in hepatic encephalopathy induced by thioacetamide in rats. Neurosci Lett 2021; 745:135617.
28. Chinopoulos C, Zhang SF, Thomas B, Ten V, Starkov AA. Isolation and functional assessment of mitochondria from small amounts of mouse brain tissue. In: Neurodegeneration: Methods and protocols. Springer; 2011. p. 311-324.
29. Lee DR, Helps SC, Macardle PJ, Nilsson M, Sims NR. Alterations in membrane potential in mitochondria isolated from brain subregions during focal cerebral ischemia and early reperfusion: evaluation using flow cytometry. Neurochem Res 2009; 34:1857-1866.
30. Caro AA, Adlong LW, Crocker SJ, Gardner MW, Luikart EF, Gron LU. Effect of garlic-derived organosulfur compounds on mitochondrial function and integrity in isolated mouse liver mitochondria. Toxicol Lett 2012; 214:166-174.
31. Niknahad H, Heidari R, Alzuhairi AM, Najibi A. Mitochondrial dysfunction as a mechanism for pioglitazone-induced injury toward HepG2 cell line. Pharm Sci 2014; 20:169-174.
32. Ghadernezhad N, Khalaj L, Pazoki-Toroudi H, Mirmasoumi M, Ashabi G. Metformin pretreatment enhanced learning and memory in cerebral forebrain ischaemia: The role of the AMPK/BDNF/P70SK signalling pathway. Pharm Biol 2016; 54:2211-2219.
33. Jalali MS, Saki G, Farbood Y, Saeed Azandeh S, Mansouri E, Dehcheshmeh MG, *et al.* Therapeutic effects of Wharton's jelly-derived mesenchymal stromal cells on behaviors, EEG changes and IGF-1 in rat model of the Parkinson's disease. J Chem Neuroanat 2021; 113:101921.
34. Dhanda S, Gupta S, Halder A, Sunkaria A, Sandhir R. Systemic inflammation without gliosis mediates cognitive deficits through impaired BDNF expression in bile duct ligation model of hepatic encephalopathy. Brain Behav Immun 2018; 70: 214-232.
35. Yan B, Liu Q, Ding X, Lin Y, Jiao X, Wu Y, *et al.* SIRT3-mediated CypD-K166 deacetylation alleviates neuropathic pain by improving mitochondrial dysfunction and inhibiting oxidative stress. Oxid Med Cell Longev 2022; 2022: 4722647.

36. Chadipiralla K, Reddanna P, Chinta RM, Reddy PVB. Thioacetamide-induced fulminant hepatic failure induces cerebral mitochondrial dysfunction by altering the electron transport chain complexes. Neurochem Res 2012; 37:59-68.
37. Jayakumar A, Panickar K, Murthy CR, Norenberg M. Oxidative stress and mitogen-activated protein kinase phosphorylation mediate ammonia-induced cell swelling and glutamate uptake inhibition in cultured astrocytes. J Neurosci 2006; 26: 4774-4784.
38. Norenberg MD. Oxidative and nitrosative stress in ammonia neurotoxicity. Hepatology 2003; 37: 245-248.
39. Bustamante J, Lores-Arnaiz S, Tallis S, Roselló D, Lago N, Lemberg A, *et al.* Mitochondrial dysfunction as a mediator of hippocampal apoptosis in a model of hepatic encephalopathy. Mol Cell Biochem 2011; 354: 231-240.
40. Norenberg M, Rao KR. The mitochondrial permeability transition in neurologic disease. Neurochem Int 2007; 50: 983-997.
41. Przedborski S, Vila M. MPTP: A review of its mechanisms of neurotoxicity. J Neurochem 2001; 1: 407-418.
42. Dagon Y, Avraham Y, Ilan Y, Mechoulam R, Berry EM. Cannabinoids ameliorate cerebral dysfunction following liver failure via AMP-activated protein kinase. FASEB J 2007; 21: 2431-2441.
43. Jafaripour L, Esmaeilpour K, Maneshian M, Bashiri H, Rajizadeh MA, Ahmadvand H, *et al.* The effect of gallic acid on memory and anxiety-like behaviors in rats with bile duct ligation-induced hepatic encephalopathy: role of AMPK pathway. Nutr Neurosci 2022; 12:425.
44. Anamika, Trigun SK. Sirtuin-3 activation by honokiol restores mitochondrial dysfunction in the hippocampus of the hepatic encephalopathy rat model of ammonia neurotoxicity. J Biochem Mol Toxicol 2021; 35: e22735.
45. Yang Y, Wang W, Tian Y, Shi J. Sirtuin 3 and mitochondrial permeability transition pore (mPTP): A systematic review. Mitochondrion 2022; 64:103-111.
46. Wang X, Gao X, Michalski S, Zhao S, Chen J. Traumatic brain injury severity affects neurogenesis in adult mouse hippocampus. J Neurotrauma 2016; 33: 721-733.
47. Ding W, Qi M, Ma L, Xu X, Chen Y, Zhang W, *et al.* ADP/ATP translocase 1 protects against an α-synuclein-associated neuronal cell damage in Parkinson's disease model. Cell Death Dis 2021; 11:1-15.
48. Klumpe I, Savvatis K, Westermann D, Tschöpe C, Rauch U, Landmesser U, *et al.* Transgenic overexpression of adenine nucleotide translocase 1 protects ischemic hearts against oxidative stress. J Mol Cell Cardiol 2016; 94: 645-653.
49. Zhang C, Jiang H, Wang P, Liu H, Su X. Transcription factor NF-kappa B represses ANT1 transcription and leads to mitochondrial dysfunctions. Sci Rep 2017; 7:44708.
50. Baek SH, Park SJ, Jeong JI, Kim SH, Han J, Kyung JW, *et al.* Inhibition of Drp1 ameliorates synaptic depression, Aβ deposition, and cognitive impairment in an Alzheimer's disease model. J Neurosci 2017; 37: 5099-5110.
51. Song Y, Li T, Liu Z, Xu Z, Zhang Z, Chi L, *et al.* Inhibition of Drp1 after traumatic brain injury provides brain protection and improves behavioral performance in rats. Brain Res 2019; 304: 173-185.
52. . Du J, Li H, Song J, Wang T, Dong Y, Zhan A, *et al.* AMPK activation alleviates myocardial ischemia-reperfusion injury by regulating Drp1-mediated mitochondrial dynamics. Front Pharmacol 2022; 13:862204.
53. Yan X, Yang Y, Huang W, Fu S, Cui B, Chu M, *et al.* Beneficial effects of the herbal medicine Zuo Gui Wan in a mice model of Alzheimer's disease via Drp1-mediated inhibition of mitochondrial fission and activation of AMPK/PGC-1α-regulated mitochondrial bioenergetics. J Ethnopharmacol 2025;119425.
54. Liu J, Yan W, Zhao X, Jia Q, Wang J, Zhang H, *et al.* Sirt3 attenuates post-infarction cardiac injury via inhibiting mitochondrial fission and normalization of AMPK-Drp1 pathways. J Mol Cell Cardiol 2019; 53: 1-13.
55. Marchenko N, Moll U. Mitochondrial death functions of p53. Mol Cell Oncol 2014; 1: e955995.
56. Mukherjee R, Tetri LH, Li SJ, Riardo G, Ostberg NP, Tsegay KB, *et al.* Drp1/p53 interaction mediates p53 mitochondrial localization and dysfunction in septic cardiomyopathy. J Mol Cell Cardiol 2023; 177: 28-37.
57. Haileselassie B, Joshi AU, Minhas PS, Mukherjee R, Andreasson KI, Mochly-Rosen D. Mitochondrial dysfunction mediated through dynamin-related protein 1 (Drp1) propagates impairment in blood brain barrier in septic encephalopathy. J Neuroinflammation 2020; 17: 1-11.
58. Milewski K, Orzeł-Gajowik K, Zielińska M. Mitochondrial changes in rat brain endothelial cells associated with hepatic encephalopathy: Relation to the blood-brain barrier dysfunction. Neurochem Res 2024; 49: 1489-1504.
59. Sun F, Si Y, Bao H, Xu S, Shi H, Zhang Y, *et al.* Regulation of sirtuin 3-mediated deacetylation of cyclophilin D attenuated cognitive dysfunction induced by sepsis-associated encephalopathy in mice. Cell Mol Neurobiol 2017; 37: 1457-1464.
60. Qi X, Qvit N, Su YC, Mochly-Rosen D. A novel Drp1 inhibitor diminishes aberrant mitochondrial fission and neurotoxicity. J Cell Sci 2013; 126:789-802.
61. Khanna A, Chakraborty S, Tripathi SJ, Acharjee A, Rao S, Trigun SK. SIRT1 activation by resveratrol reverses atrophy of apical dendrites of hippocampal CA1 pyramidal neurons and neurobehavioral impairments in moderate grade hepatic encephalopathy rats. J Chem Neuroanat 2020; 106:101797.